

# Hydronium Ion Diffusion in Model Proton Exchange Membranes at Low Hydration: Insights from Ab Initio Molecular Dynamics

## Supporting Information

Tamar Zelovich<sup>(1)</sup>, Karen I. Winey<sup>(2)</sup>, and Mark E. Tuckerman<sup>(1),(3),(4)\*</sup>

- 1) Department of Chemistry, New York University (NYU), New York, New York 10003, United States
- 2) Department of Materials Science and Engineering, University of Pennsylvania, Philadelphia, Pennsylvania 19104, United States
- 3) Courant Institute of Mathematical Sciences, New York University (NYU), New York, New York, 10012, United States
- 4) NYU-ECNU Center for Computational Chemistry at NYU Shanghai, 3663 Zhongshan Rd. North, Shanghai, 200062, China

### Systems Parameters

Table S1: System parameters for the two graphane bilayer structures presented in this study.

System	$\lambda$	Effective Water Density (gr/cm <sup>3</sup> )	Cation Spacing (Å)		Cell Geometry (Å)		
			$\Delta x$	$\Delta y$	x-axis	y-axis	z-axis
$\lambda 3$	3	0.261	10	6.6	10	13	7.3
$\lambda 4$	4	0.326	10	6.6	10	13	7.3

For each system, the effective water density is estimated by  $\rho = \frac{m_{\text{H}_2\text{O}}[\text{gr}]}{(V_{\text{cell}} - V_{\text{SO}_3^-})[\text{Å}^3]}$ , in which the effective volume in the denominator is obtained by subtracting the volume of the anions,  $V_{\text{SO}_3^-}$  (estimated by the size of the anion in its initial configuration) from the volume between the two graphane sheets,  $V_{\text{cell}}$ .<sup>1</sup>

## Radial Distribution Functions

In Figure S1a, we present the OO RDF, in which O represents all oxygens in the system but the  $\text{SO}_3^-$  oxygens. The first peak is located at 2.7 Å and 2.6 Å for systems  $\lambda 3$  and  $\lambda 4$ , respectively. This minor shift to the left for system  $\lambda 4$  can be explained by the uniform water distribution seen for this system, as it results in a higher water density, which can lead for a shorter OO bond. In Figure S1b, we present the OO RDF, in which O represents all oxygens in the system. We find there are two peaks in the first solvation shell. The first peak, at 2.5 Å, corresponds to the OO of  $\text{SO}_3^-$  oxygens, and the second peak, at 2.8 Å, corresponds to the water oxygens.

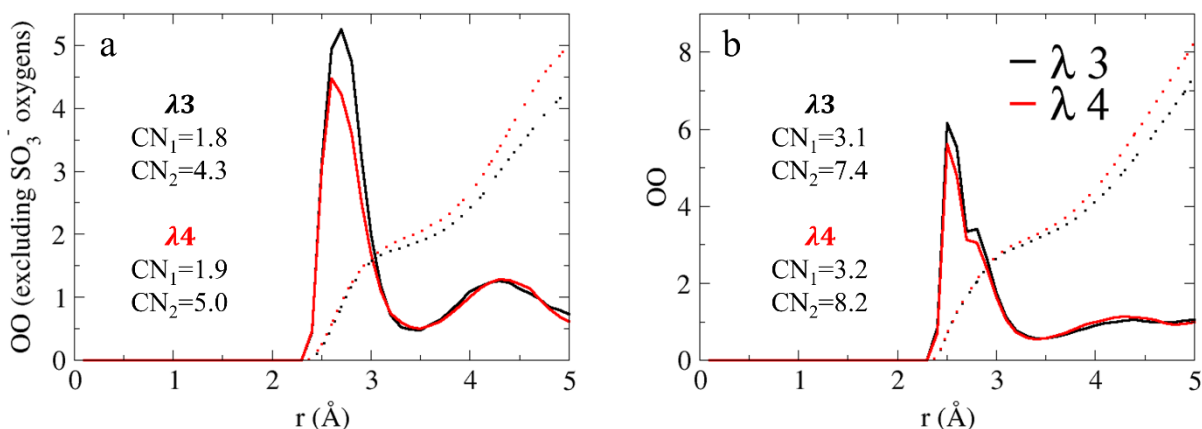


Figure S1: Radial distribution functions for systems  $\lambda 3$  and  $\lambda 4$  (black and red curves, respectively) of OO (a) O represents all oxygens in the system, but the  $\text{SO}_3^-$  oxygens, and (b) O represents all oxygens in the system. The colored dotted lines and the inset of both figures represent the obtained coordination numbers.

In Figure S2a, we present the  $\text{O}_s\text{O}_w$  RDF and CNs, in which  $\text{O}_s$  represents both  $\text{SO}_3^-$  and  $\text{SO}_3\text{H}$  oxygens. The first peak is located at 2.8 Å for both systems. We find that the CN values of both the first and second solvation of systems  $\lambda 3$  and  $\lambda 4$  are similar to the values presented in Figure 4 of the main text. These results suggest that the oxygens of the sulfonate are mainly solvated by water oxygens. In Figure S2b, we present the  $\text{O}^*\text{O}_w$  RDF, in which  $\text{O}^*$  represents both  $\text{H}_3\text{O}^+$  and  $\text{SO}_3\text{H}$ . The first peak is located at 2.6 Å for both systems, with CN values of 1.85 and 2.0 for the first peak, and 4.1 and 4.7 for the second peak, for systems  $\lambda 3$  and  $\lambda 4$ ,

respectively. A comparison with the results presented in Figure 3 of the main text reveals that the oxygens of the sulfonate contribute significantly to the first and second solvation shells of the hydronium.

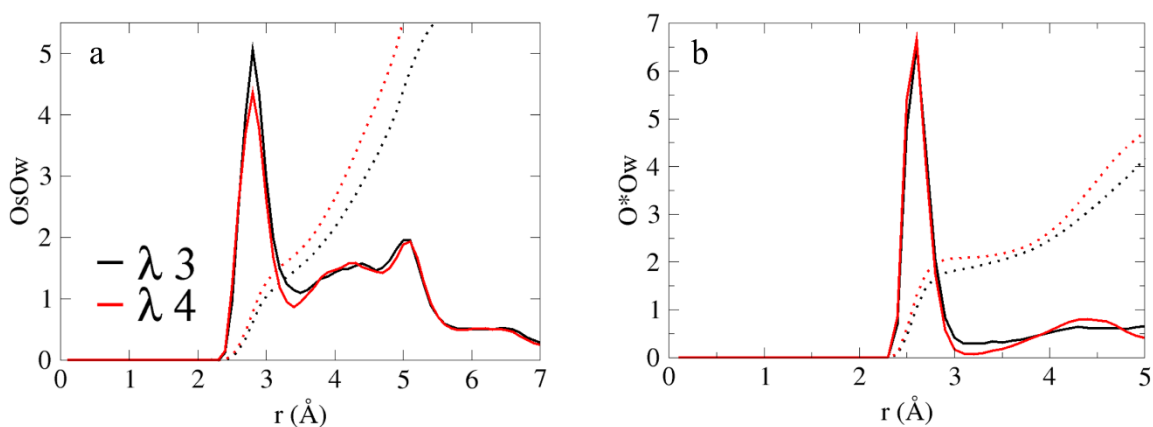


Figure S2: Radial distribution functions for systems  $\lambda 3$  and  $\lambda 4$  (black and red curves, respectively) of (a)  $O_s O_w$ , where  $O_s$  represents both  $SO_3^-$  oxygens and  $SO_3H$  and (b)  $O^* O_w$ , where  $O^*$  represents both  $H_3O^+$  and  $SO_3H$ . The colored dotted lines and the inset of both figures represent the obtained coordination numbers.

### Hydronium Ion Oxygen Coordinates

To understand the underlying differences in diffusion constants and to present a complete analysis of the mechanisms hydronium transport, we plot the coordinates of the hydronium oxygens in each system as a function of time along the  $x$ - and  $y$ -axes separately in Figure S3 (the hydronium ion coordinates along the  $z$ -axis are not presented as they contribute negligibly to the overall diffusion). In addition, we label proton transfer (PT) events (including events in which the proton transfers forth and back before transferring to a third oxygen, which are referred to as “rattling” events) with gray lines, where each line represents a change in the identity of the hydronium oxygen. It should be noted, that the relatively high number of PT events seen between the hydronium ion and water oxygens in its first and second solvation shells for system  $\lambda 4$ , do not contribute to the overall diffusion, as most of the PT events are considered at rattling events. We assume the increasing number of rattling events seen in system are a result of the stable water and hydronium complexes obtained in the system. Exploring the trajectory, suggest

that most of the rattling events are a result of proton hopping between the hydronium ions and the  $\text{SO}_3^-$  oxygens. seen rattling events

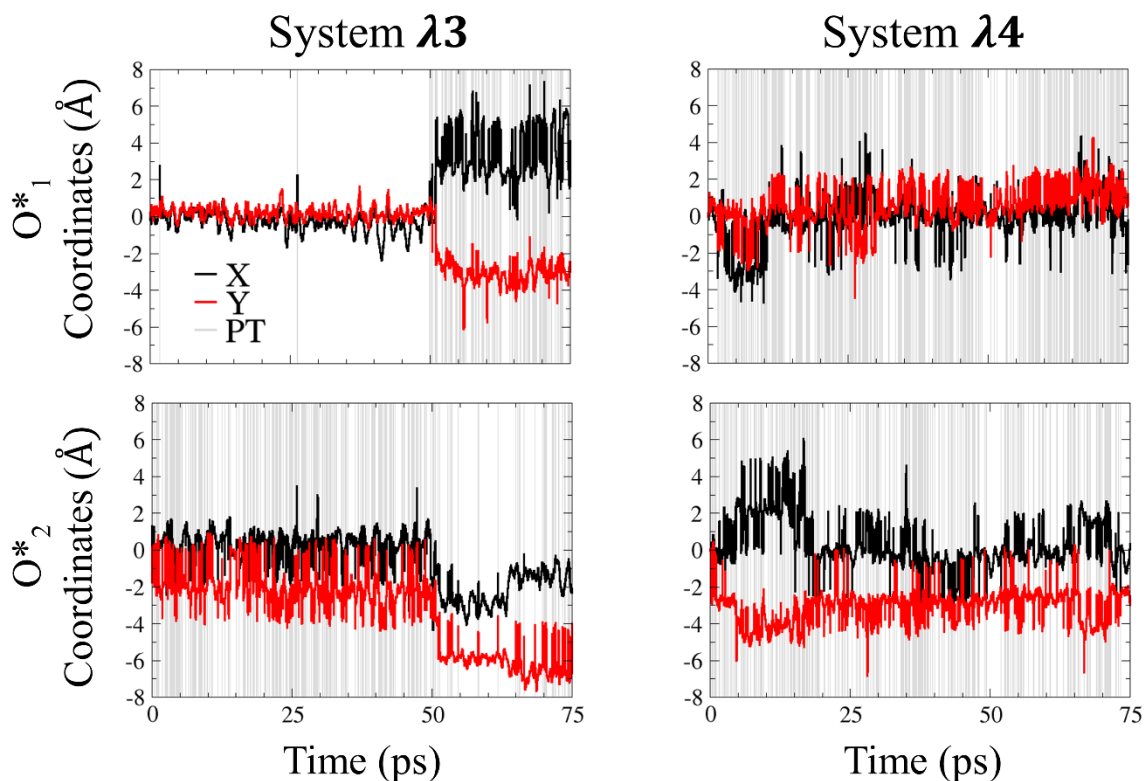


Figure S3: Hydronium ion oxygen coordinates as a function of time (black and red curves for  $x$  and  $y$  coordinates, respectively) for  $\text{O}^*_1$  and for  $\text{O}^*_2$  during the simulations for systems  $\lambda 3$  and  $\lambda 4$ . Gray lines indicate PT events (including rattling).

### Mean Square Displacements

Figure S4 presents the mean square displacement (MSD) curves as functions of time, calculated for each of the three spatial directions separately and as an average over the three directions, for the two systems in the main text. The results were used for the calculation of the diffusion constants presented in the main text. In all systems, the results presented were obtained from the first 10% of the NVE trajectory in order to show the transition to the diffusive-linear behavior appears approximately after 2ps. However, for the diffusion calculation, the data used was obtained from the first 2% to the first 10% of the NVE trajectory.

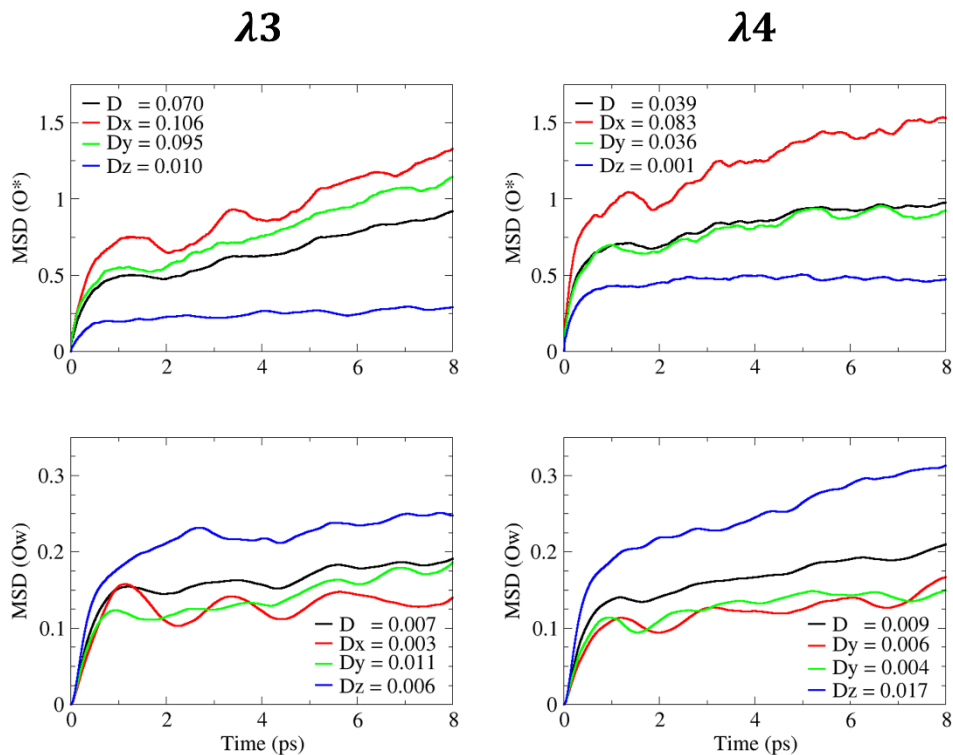


Figure S4: Mean square displacement (MSD) for  $\text{OH}_3^+$  (upper panels) and  $\text{H}_2\text{O}$  (lower panels) as a function of time, calculated as an average (black curve) and for each of the axes separately (red, green and blue represents  $x$ -,  $y$ - and  $z$ - axes, respectively) for the two systems.

### Population Probabilities of Different O\* Solvation Complexes

The hydrogen bond (HB) criteria obtained from the OO and O\*H RDF results are as follows: the distance between the oxygen  $\text{O}_a$  of HB acceptor and the hydrogen  $\text{H}_d$  and HB donor  $R_{\text{O}_a\text{H}_d} < 2.5 \text{ \AA}$ , the distance between the oxygen  $\text{O}_a$  and oxygen  $\text{O}_d$  of HB donor  $R_{\text{O}_a\text{O}_d} < 3.5 \text{ \AA}$ .

	3A+0D	4A+0D
$\lambda 3$	90.4	8.4
$\lambda 4$	86.4	12.8

**Figure 5 of the main text: The time in percentage the hydronium ions spent as  $\text{SO}_3^-$  and  $\text{SO}_3\text{H}$**

In order to calculate the percentage of time presented in Figure 5 of the main text, we first uniquely assign, at each point along the trajectory, every hydrogen to an oxygen atom and then determine which oxygens belong to water molecules and which are the cores of hydronium ions. We also determine whether the anionic end group appears as  $\text{SO}_3^-$  or  $\text{SO}_3\text{H}$ . We then count the number of times the end group appears as  $\text{SO}_3\text{H}$  along the trajectory and divide it by  $2N_{\text{step}}$ , where the factor of 2 counts the two hydroniums, and  $N_{\text{step}}$  is the number of steps in the NVE trajectory.

**References**

- [1] T. Zelovich, L. Vogt-Maranto, M. Hickner, S.J. Paddison, C. Bae, D.R. Dekel, M.E. Tuckerman, “Hydroxide Ion Diffusion in Anion Exchange Membranes at Low Hydration: Insights from Ab initio Molecular Dynamics,” *Chem. Mater.*, 31, 5778–5787, 2019.